Computational Modeling of Mixing and Gasification in Continuous-Flow Supercritical Water Reactor

Kartik Tiwari, Brian Pinkard, David Gorman, Justin Davis, John Kramlich, Per Reinhall, Igor Novosselov*
Department of Mechanical Engineering, University of Washington, Seattle, USA
* Corresponding author e-mail: ivn@uw.edu

ABSTRACT:

Supercritical water (sc-H_2O) reactors have been used for both biomass gasification and the destruction of hazardous waste. Laboratory scale reactors are typically used to develop chemical kinetic rate parameters; these smaller reactors are operated at low Reynolds numbers and thus may suffer from slow mixing between the reagent and sc-H_2O. This slow mixing rate may introduce errors into the derived chemical kinetic rate parameters. In this study, we investigate a multiple-jet in crossflow mixing section, which enables rapid mixing of reagents into sc-H_2O. A parametric analysis establishes an optimum jet to crossflow velocity ratio (*R)* for scalar mixing using 3D computational fluid dynamics (CFD) simulations. Kinetic theory modeling was used to calculate the physical properties of the fluids at the supercritical state; these predictions were compared against data available in published literature. CFD simulations show that mixing can be characterized by three distinct regimes: (i) under-penetrating jets, (ii) jets forming counter-rotating vortices (CRV), and (iii) impinging jets. The best mixing performance is observed for jets forming CRV, while under-penetrating jets show the poorest mixing. Decomposition of methanol (MeOH) in a continuous-flow reactor is simulated using a global first-order chemical kinetic rate calculated from published data. This numerical modeling sheds insight into organic compound decomposition, and it can be used in industrial process optimization.

NOMENCLATURE

R = Velocity ratio of jet to crossflow
D_{ij} = Diffusion coefficient
T = Temperature
M_w = Molecular weight
ρ = Density
σ = Lennard Jones energy parameter
Ω_D = Diffusion collision integral
μ = Viscosity
Ω_μ = Viscosity collision integral
ϕ = Mass fraction of scalar
$\vec{v}$ = Velocity
U = Mean velocity
A = Area
t = Time
Y = Mass fraction of the species
d_c = Diameter of main pipe
j = Diffusion flux
τ_d = Characteristic diffusion time
Subscript p,q = Property of p^{th} or q^{th} species
Subscript k = Value at the k^{th} control area
Subscript j = Jet parameters
Subscript c = Crossflow parameters

INTRODUCTION

Supercritical water reactors have been used for biomass gasification and the destruction of toxic organic waste. These reactors exist in batch as well as continuous flow configurations. Continuous-flow sc-H_2O reactors provide better process control, higher throughput, and scalability with reduced experimental time over batch reactors. Many reactors use a premixed slurry of water and the organic reagent, but this can lead to the formation of char in the heating section [1]. In chemical kinetic studies, the ambiguity about the reaction onset in a multi-temperature experiment also introduces uncertainty in both determining the reaction residence time and in identifying the temperature dependence of the rate constants. Post-critical mixing, where reagents are mixed into water already above the critical point, can suffer from mixture non-homogeneity, especially in small-scale reactors due to low Reynolds number flows [2]. Several passive and active mixing systems have been proposed for rapid mixing of fluids in such small-scale reactors.

Reviews of microscale mixing systems[3] show that jet-based systems are preferred due to the simplicity of design, fast mixing, and reduced cost; the mixing is improved by inducing turbulence and increasing the diffusion surface area between the fluid streams [3].

A multiple-jets-in-crossflow (MJC) mixer consists of radially symmetric jets perpendicular to a tube or duct carrying the bulk flow. Such mixers are used in many engineering applications, such as the production of nanoparticles, and pyrolysis of hydrocarbons [4, 5]. Extensive numerical and experimental studies describe the dynamics of flow structures and large-scale mixing for a single jet in crossflow [6-9]. Non-dimensional parameters defining jet behavior in crossflow are momentum ratio (J) and velocity ratio (R).

$$J = \frac{\rho_j U_j^2}{\rho_c U_c^2} \tag{1}$$

$$R = \frac{U_j}{U_c} \tag{2}$$

The interaction of the jet with the crossflow leads to the formation of large-scale vortex structures like counter-rotating vortices (CRV), horseshoe, and hairpin vortices affecting jet mixing with the cross-flow [6, 10]. Experiments and numerical simulations show that scalar mixing for multiple jets in a cylindrical crossflow depends on the J or R parameters [11-14]. Most studies focus on mixing of fluids with well-defined properties and at moderate to large Re numbers. Because the mixing rate depends on fluid properties, it is necessary to evaluate the performance of MJC for (i) supercritical fluid reactors and (ii) in a laminar and transitional (to turbulent) regions.

Interest in gasifying organic compounds has prompted research into the decomposition mechanisms and reaction rates of organic compounds in sc-H_2O. Simple alcohols have been studied as surrogates for liquid intermediates, and by-products in the decomposition of more complex molecules [15]. Reforming alcohols in sc-H_2O to produce hydrogen may also find an application in automotive fuel cells [16-19]. The scientific literature does not present a robust methodology for numerical modeling of organic compound decomposition in sc-H_2O. Limited modeling studies have focused on predicting equilibrium composition and the development of global chemical kinetic rates [20, 21]. However, CFD modeling has been extensively used in combustion science to predict complex processes involving mixing/chemistry interactions, and the reduction of complex mechanisms into global representations for industrial applications, e.g., [22-25]. Applying such modeling techniques in supercritical systems (not limited to water) can guide the design and improvement of existing and new reactor designs.

In this study, we investigate mixing and decomposition of organic compounds in an sc-H_2O reactor using finite volume CFD modeling. The kinetic theory model is evaluated for calculating the binary diffusion coefficients and viscosity of the fluids in their supercritical state. These properties are then incorporated into a CFD analysis to design an MJC mixing section for a laboratory reactor. The decomposition of MeOH is based on first-order kinetic rates obtained using experimental data from literature [26].

NUMERICAL METHODS:

Kinetic theory model

To model the interaction between the reactants, it is essential to accurately estimate the physical and transport properties of the fluids in the supercritical state. These properties can vary significantly with temperature, pressure [27, 28]. Kinetic theory can provide an adequate estimate for some engineering applications, however, the accuracy of the kinetic theory for supercritical fluids needs verification. Here the applicability of kinetic theory to predict the binary diffusion coefficient and viscosity of benzene in water is evaluated in the supercritical region. Benzene is one of the intermediates in the SCW decomposition of lignin, cellulose, glucose, and biomass [29]. Conveniently, experimental data for the binary diffusion coefficient [27] and kinetic theory parameters [30] have been presented in the literature. The binary diffusion coefficient is calculated from the modified Chapman-Enskog equation (3).

$$D_{pq} = 0.00188 \times \frac{\left[T^3\left(\frac{1}{M_{w,p}}+\frac{1}{M_{w,q}}\right)\right]^{1/2}}{\rho\sigma_{pq}^2\Omega_D}. \quad (3)$$

Equation 4 provides viscosity formulation from the kinetic gas theory for spheres using the Lennard-Jones potential function. It is assumed that the viscosity is independent of pressure and only binary elastic collisions occur between the molecules.

$$\mu_p = 2.67 \times 10^{-6} \frac{\sqrt{M_{w,p}T}}{\sigma_p^2\Omega_{\mu,p}}. \quad (4)$$

Table 1 compares the binary diffusion coefficient of a supercritical benzene-water mixture calculated by kinetic theory and those reported by Nieto-Draghi et al. at similar operating conditions [27]. The calculated viscosity of water is compared with the NIST database [31]. The predicted and the published properties are the same order magnitude. For the lower pressure case, the data and theoretical calculations for both diffusion coefficient and viscosity agree better than in the higher pressure case. At higher pressures, the decrease in the intermolecular distance influence other molecules on the intermolecular collisions significantly, deviating from the kinetic theory assumptions. The introduction of additional tuning parameters into the kinetic theory calculations to account for pressure, ionic interactions, etc. can improve the model accuracy for supercritical fluids. However, comprehensive data sets to validate such approaches have not been developed. This task is beyond the scope of this manuscript but will be considered as a future research direction. Since the operating pressure for most sc-H_2O reactors is less than 55 MPa, the kinetic theory model can be used for CFD modeling. However, more robust experimental data and analytical modeling are required to generalize these conclusions. In this study, the diffusion coefficient and the viscosity of the fluids will be modeled using kinetic theory.

Table 1. Comparison of the binary diffusion coefficient and viscosity of water with the published properties [27, 31]. Benzene mole-fraction - 0.1

Pressure (MPa)	Temp (K)	Diffusion coefficient from Nieto-Draghi [27] (m^2/s)	Diffusion coefficient by kinetic theory (m^2/s)	Viscosity from NIST database [31] (μPa×s)	Viscosity predicted by kinetic theory (μPa×s)
55.29	673	3.2 ×10E-8	5.81 ×10E-8	77.31	29.51
686.11	673	1.1 ×10E-8	0.48 ×10E-8	130.00	29.51

Multiple-Jets-in-Crossflow Mixer Geometry

Three-dimensional CFD analysis is used to study the mixing of supercritical fluids in an MJC mixer. Figure 1 shows a schematic of the design. The numerical grid consists of ~2 million tetrahedral elements. The maximum cell skewness is maintained below 0.85. Six prism layers (inflation layers) are maintained along the flow near the wall to model the boundary layer dynamics accurately. The sc-H_2O flows at 2.19 kg/s through a tube of ID 3.05 mm. The benzene (10% by mass relative to the water) is injected through the four perpendicular round inlets with the diameter of the injection tubes being varied. Both fluids are injected at supercritical conditions (923 K and 25 MPa). The densities are taken from the NIST database whereas the viscosities and diffusion coefficients are calculated by kinetic theory. Transient CFD solves the 3D Naiver–Strokes, energy, and species transport equations [32]. The delayed detached eddy simulation (DDES) is used to model flow instabilities and potential transition to turbulence at high jet velocities [33]. DDES resolves large scales of turbulence with LES schemes and uses RANS type schemes to model sub-grid scales.

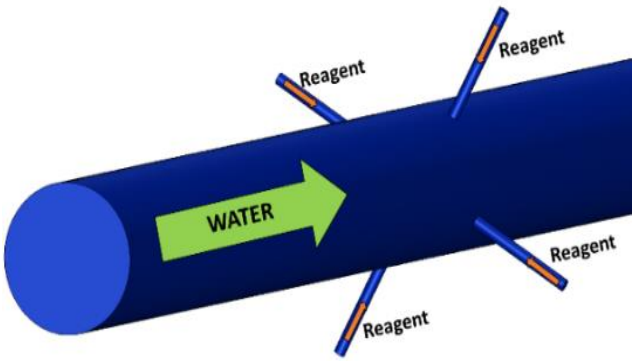

Figure 1. Schematic for multiple jets in a crossflow mixer with four jets used in this study.

Methanol Decomposition Study

The experimental data of Hack et al. for MeOH decomposition [26] is used to derive the rate parameters. The authors provide MeOH concentration data over a range of temperatures and residence times and suggest that MeOH decomposition can be modeled with the overall global reaction given by (5). The reaction rate was independent of the initial MeOH concentration in the mass fraction range of 0.002 to 0.004.

$$CH_3OH + H_2O \rightarrow CO_2 + 3H_2 \tag{5}$$

Based on the data [26], we calculated an activation energy and pre-exponential constant of 147.96 kJ/mole and 1.94E+10 s^{-1} respectively; these rate parameters are used in CFD. Equation 3 is used to calculate the binary diffusion coefficient while other fluid properties are taken from the NIST database.

RESULTS

Optimization of the Mixing Section

Table 2. Jet parameters used for all simulations

Case	Velocity ratio (*R*)	Jet inlet diameter (mm)	Jet Re	Jet trajectory
1	0.22	0.60	670	Under-penetrating jets
2	1.26	0.25	1609	CRV Jets
3	2.73	0.17	2367	
4	10.00	0.09	4526	Impinging Jets

The results of the CFD simulations for mixing water and benzene in an MJC mixer are presented in this section. The mixing rate and the large-scale flow features depend on the momentum flux ratio (*J*) [6, 11, 13]. For all the simulations, the density of the fluids is constant, and *J* can be expressed as *R*. For a constant mass flow rate of jet and crossflow, the diameter of jets is varied to study the influence of *R* on the mixing rate and the large-scale flow features. Table 2 summarizes the jet characteristics for each simulation. The jet diameter varied 0.1 - 0.6 mm, *Re* =670 - 4023, covering the laminar and transitional flow regimes. To understand the mixing process, it will be useful to revisit the basic principles of mixing. Fick's law gives the diffusion flux transfer of a species per unit area (6).

$$j_p = -D_{pq}\nabla Y_p. \tag{6}$$

By re-arranging (6), the characteristics diffusive flux can be expressed as [3]:

$$\frac{1}{\tau_{d,p}} = D_{pq} \cdot A_{pq} \cdot \nabla Y_p. \tag{7}$$

Equation 7 gives the characteristic diffusion time for any species, where "A" is the diffusion area between the two fluids. The diffusion rate improves with the increase in contact area, diffusion coefficient, and concentration gradient. Equation 8 gives the uniformity index (UI). This is a measure of mixing uniformity, representing a variance in the species concentration, weighed by mass flux, over the cross-section of the flow. UI values close to unity represent a homogeneously mixed state, and values close to zero indicate segregated flow.

$$UI = 1 - \frac{\sum_{k=1}^{n}[(|Y_k - Y|)(|\rho_k \overrightarrow{v_k} A_k|)]}{2|Y| \times \sum_{n}^{k}(|\rho_k \overrightarrow{v_k} A_k|)}. \tag{8}$$

Figure 2 (a) shows the path-lines originating from the jet inlet withthe axial vorticity contours at 100mm from the injection plane (end-view from water inlet). The flow pattern can be characterized as: (i) under-penetrating jets, (ii) jets forming CRV, and (iii) impinging jets.

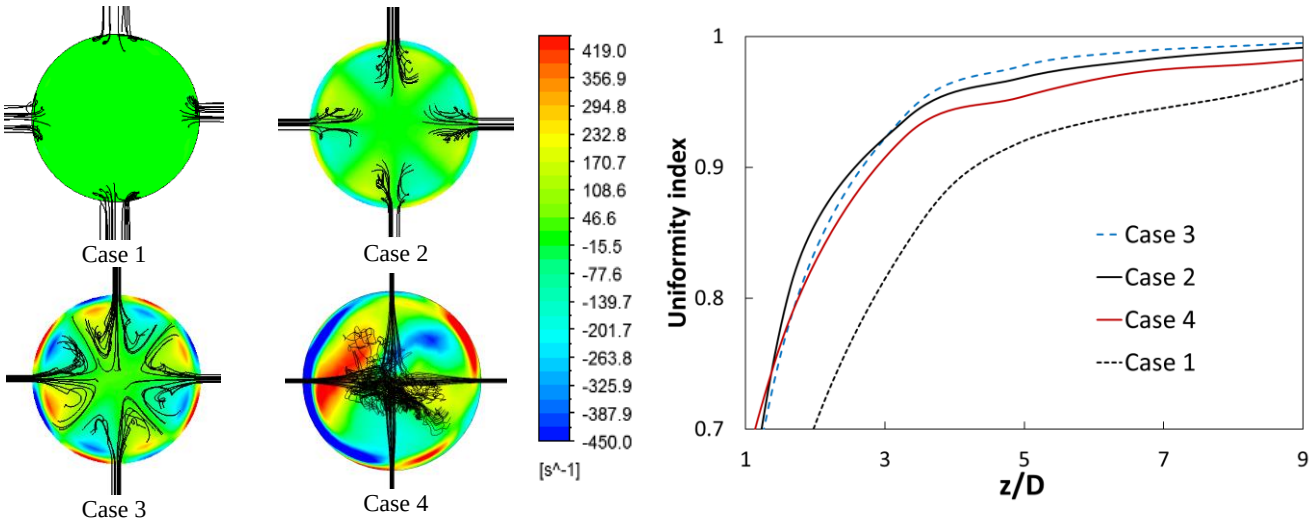

Figure 2. (a) Path-lines of flow (in black) originating at jet inlets along with the instantaneous vorticity contour at a cross section 10 cm from the jet inlet for specified jet parameters. The strength of counter-rotating vortices increases with the velocity ratio until the jets impinge and make the flow chaotic. (b) UI along the dimensionless axial distance for the jet with specified momentum ration. The jets forming CRV leads to the fastest mixing.

For a given geometry, jets underpenetrate for lower *R* values (Case 1) as the momentum of the jets is not enough to penetrate the crossflow. The fluid from the jet is trapped in the boundary layer of the crossflow and does not result in significant flow vorticity (see colored vorticity contours). The results are consistent with the direct numerical simulation (DNS) study by Rau and Mahesh for a single jet in crossflow, which shows no coherent vortex ring formation for $R<2$ [34]. The jets penetration improves with increased *R*. For cases 2 and 3, CRVs are observed downstream of the jets; the mixing rates for these cases are similar. The increased velocity ratio does not improve the diffusion area but increases the strength of CRV. However, for case 4, the jets have enough momentum to penetrate the crossflow and impinge at the center, making the flow turbulent. No CRVs are observed, as the jets lose their initial vorticity after the collision and behave similar to a point momentum source at the impingement location. Momentum displacement and turbulent diffusion allow the reagent to mix with the bulk flow in all directions moving away from the impingement region, and eventually to be carried downstream by the bulk flow. This locally turbulent jet can relaminarize if the pipe *Re* is laminar. Figure 2 (b) shows the UI of benzene vs. the non-dimensional axial distance. For case 1 the jets underpenetrate, and mixing is slowest as the diffusion area between the fluids is the lowest. CRV forming jets show the best mixing due to the high contact area. The mixing rate for impinging jets is slower than the jets forming CRV as the impingement of jets forms a single stream of benzene in the center instead of four streams as in case 2 and case 3 with CRV. Optimum mixing in the MJC mixer occurs at flowrates and jet diameters that promote CRV structures.

Decomposition Simulations of Methanol in Supercritical Water

The first-order chemical kinetics derived from literature data, as described above [26], were used in a CFD calculation to observe the influence of finite rate mixing on the decomposition rate of methanol. Table 3 shows the conditions used in the CFD simulation. The low *Re* suggests laminar bulk flow conditions for all cases. MeOH is injected from four radial orifices, each with a 0.25 mm internal diameter. Due to the flow symmetry is shown in Figure 1, we adopt a computational domain that consists of a quadrant section of the 3D domain. Domain length is based on the residence time required to fully decompose MeOH at each temperature. Figure 3(a) compares the MeOH decomposition rate predicted by CFD with

Table 3. The boundary condition for modeling MeOH decomposition

Average Temp in the Reactor (K)	Mass Flow Rate of Water (g/s)	Residence Time (s)	Reynold's Number
653	0.058	100.0	384
683	0.042	94.3	422
719	0.050	21.6	652

the premixed data that are uninfluenced by mixing. The normalized concentration of MeOH for the CFD is evaluated at various cross-sections of the domain corresponding to the experimental residence times for each temperature. $[CH_3OH]_0$ is the initial concentration of MeOH at the injection plane. The predicted MeOH concentration is in close agreement with the experimental data, which indicates that the overall MeOH destruction is not influenced by finite-rate mixing under these conditions. The principal reason for this is that the chemical rate is relatively slow compared to the mixing rate. The effect of the mixing rate on the overall reaction can, however, be significant for slow mixing and fast chemical rates. The relationship between the mixing and kinetic rates can be described by the global and local Damkohler (Da) and Karlovitz (Ka) numbers, which are often used in combustion modeling, e.g., [35]. In the CFD simulations, the competition between the mixing and chemical kinetic rates in the presence of turbulence can be evaluated using a model describing turbulence-chemistry interaction, e.g., the eddy-break-up model or the eddy dissipation concept as presented in combustion literature [36, 37]. Figure 3(b) shows the normalized concentration and UI as a function of residence time in the reactor. The mixing rate is significantly faster than the decomposition rate of MeOH in sc-H_2O, especially at the lower temperatures. UI reaches 90% in less than 2 secs, while for rates based on Hack et al. data, it takes more than 30 secs for 50% decomposition at 683 K and 10 sec at 653 K. However, at 719 K, the reaction rate of MeOH becomes comparable to the mixing rate.

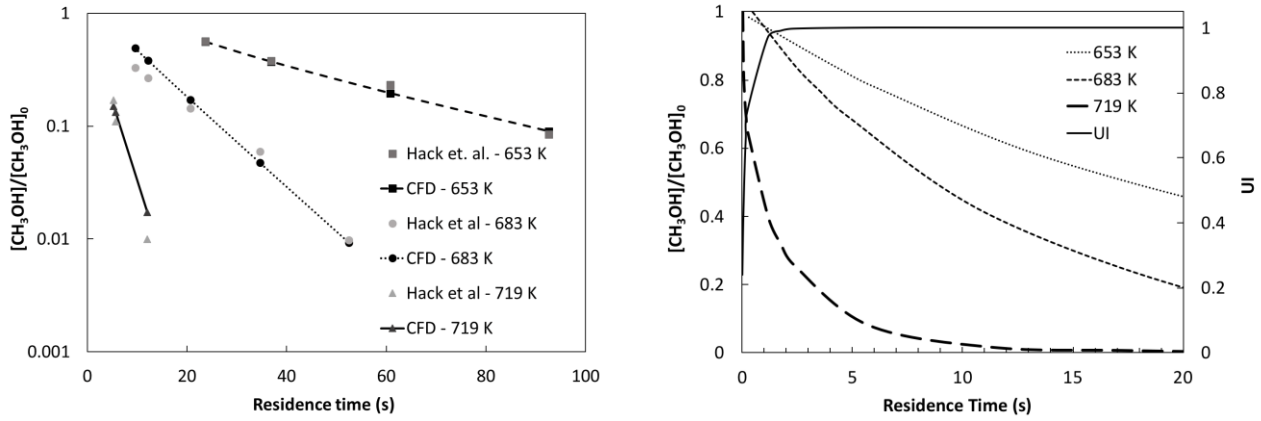

Since 50% of the MeOH is reacted at UI~0.8, the plug flow assumptions are not valid in this operational condition. An experimentally determined reaction rate at such conditions can be considerably affected by

Figure 3. (a) MeOH decomposition at different reactor temperatures from CFD compared with the data [26]. (b) Uniformity Index and the MeOH concentration vs. the residence time in the reactor. The mixing time is approximately 1 s, which is significantly less than the characteristic chemical time.

the mixing rate. The decomposition rate of MeOH in sc-H_2O is moderate compared to other organic molecules. For example, the reaction rate of glucose and glycerol are an order magnitude greater than for MeOH [29]. Therefore, for high temperatures and compounds with rapid decomposition, the mixing section design becomes critical.

CONCLUSIONS:

The mixing and decomposition of organic compounds in supercritical water have been studied with CFD. The kinetic theory was used to evaluate the diffusion coefficient and viscosity of a benzene and water mixture. The model shows good agreement with published properties for 55 MPa, allowing its use in practical applications. The mixing of supercritical fluids in an MJC mixer was studied using DDES CFD simulations. The velocity ratio of the jets to crossflow was varied by changing the diameter of the jets. The best mixing occurs at an optimum velocity ratio when jets form CRV downstream of the injection location. Low velocity-ratios give slow mixing as the jets under-penetrate the bulk flow. At higher velocity

ratios, the jets impinge, resulting in the formation of a single jet and reducing the available diffusion surface area. Decomposition of MeOH was modeled. The model shows good agreement with the experimental data. With MJC the mixing rate was considerably faster than the decomposition rate of MeOH at lower temperatures. At higher temperatures, the kinetic rate becomes comparable to the mixing rate. Plug flow assumptions may not be valid in situations of slow mixing and fast chemical kinetic rates. For such scenarios, the mixing section should be carefully designed for fast mixing. The computational modeling approach described can be used for the design and optimization of supercritical fluids reactors.

ACKNOWLEDGMENTS:
The author would like to recognize the funding provided by the DOD Defense Threats Reduction Agency – Grant HDTRA1-17-1-0001, as well as the resources provided by the University of Washington that made this work possible.

REFERENCES:

1. Marrone, P.A. and G.T. Hong, *Corrosion control methods in supercritical water oxidation and gasification processes.* The Journal of Supercritical Fluids, 2009. **51**(2): p. 83-103.
2. Helling, R.K., *Oxidation Kinetics of Simple Compounds in Supercritical Water: Carbon Monoxide, Ammonia and Ethanol*. 1986, MIT. p. 270.
3. James, G., H. Arne, and K. Aman, *A review of passive and active mixing systems in microfluidic devices.* International Journal of Multiphysics, 2007. **1**(1).
4. Ktalkherman, M. and I. Namyatov, *Pyrolysis of hydrocarbons in a heat-carrier flow with fast mixing of the components.* Combustion, Explosion, and Shock Waves, 2008. **44**(5): p. 529-534.
5. Kartaev, E., et al., *An Experimental Study of the Synthesis of Ultrafine Titania Powder in Plasmachemical Flow-Type Reactor.* Int. J. Chem. React. Eng., 2014. **12**(1).
6. Mahesh, K., *The Interaction of Jets with Crossflow.* Annu. Rev. Fluid Mech., 2013. **45**: p. 379-407.
7. Yuan, L.L., R.L. Street, and J.H. Ferziger, *Large-eddy simulations of a round jet in crossflow.* Journal of Fluid Mechanics, 1999. **379**: p. 71-104.
8. Su, L.K. and M.G. Mungal, *Simultaneous measurements of scalar and velocity field evolution in turbulent crossflowing jets.* J. Fluid Mech., 2004. **513**: p. 1-45.
9. Karagozian, A.R., *The jet in crossflow.* 2014.
10. Sau, R. and K. Mahesh, *Passive scalar mixing in vortex rings.* J. Fluid Mech., 2007. **582**: p. 449-461.
11. Holdeman, J.D., et al., *Mixing of multiple jets with a confined subsonic crossflow .1. Cylindrical duct.* J. Eng. Gas. Turbines Power-Trans. ASME, 1997. **119**(4): p. 852-862.
12. Luo, P., et al., *An experimental study of liquid mixing in a multi-orifice-impinging transverse jet mixer using PLIF.* Chemical Engineering Journal, 2013. **228**: p. 554-564.
13. Luo, P.C., et al., *Turbulent Characteristics and Design of Transverse Jet Mixers with Multiple Orifices.* Ind. Eng. Chem. Res., 2016. **55**(32): p. 8858-8868.
14. Urson, M.F., M.J. Lightstone, and H. Thomson, *A Numerical Study of Jets in a Reacting Crossflow.* Numerical Heat Transfer, Part A: Applications, 2001. **40**(7): p. 689-714.
15. Reddy, S.N., S. Nanda, and J.A. Kozinski, *Supercritical water gasification of glycerol and methanol mixtures as model waste residues from biodiesel refinery.* Chemical Engineering Research and Design, 2016. **113**: p. 17-27.
16. DiLeo, G.J. and P.E. Savage, *Catalysis during methanol gasification in supercritical water.* The Journal of Supercritical Fluids, 2006. **39**: p. 228-232.
17. Boukis, N., et al., *Methanol reforming in supercritical water.* Industrial and Engineering Chemistry Research, 2003. **42**(4): p. 728-735.

18. Boukis, N., et al., *Methanol Reforming in Supercritical Water for Hydrogen Production.* Combustion Science and Technology, 2007. **178**: p. 467-485.
19. van Bennekom, J.G., et al., *Reforming of methanol and glycerol in supercritical water.* The Journal of Supercritical Fluids, 2011. **58**(1): p. 99-113.
20. Srisiriwat, N. and C. Wutthithanyawat, *Thermodynamic analysis of hydrogen production from methanol reforming in supercritical water*. 2014. p. 99-104.
21. Tushar, M.S.H.K., A. Dutta, and C. Xu, *Simulation and kinetic modeling of supercritical water gasification of biomass.* International Journal of Hydrogen Energy, 2015. **40**(13): p. 4481-4493.
22. Karalus, M.F., et al., *A Skeletal Mechanism for the Reactive Flow Simulation of Methane Combustion.* 2013: p. V01BT04A065.
23. Novosselov, I.V. and P.C. Malte, *Development and Application of an Eight-Step Global Mechanism for CFD and CRN Simulations of Lean-Premixed Combustors.* 2007: p. 769-779.
24. Novosselov, I.V., *Chemical reactor networks for combustion systems modeling*. 2006, University of Washington.
25. Novosselov, I., et al. *Chemical reactor network application to emissions prediction for industial dle gas turbine*. in *ASME turbo expo 2006: Power for land, sea, and air*. 2006. American Society of Mechanical Engineers.
26. Hack, W., D. Masten, and S.J. Buelow, *Methanol and ethanol decomposition in supercritical water.* Z. Phys. Chemie-Int. J. Res. Phys. Chem. Chem. Phys., 2005. **219**(3): p. 367-378.
27. Nieto-Draghi, C., et al., *Dynamical and structural properties of benzene in supercritical water.* The Journal of Chemical Physics, 2004. **121**(21): p. 10566-10576.
28. Plugatyr, A. and I.M. Svishchev, *Molecular Diffusivity of Phenol in Sub- and Supercritical Water: Application of the Split-Flow Taylor Dispersion Technique.* The Journal of Physical Chemistry B, 2011. **115**(11): p. 2555-2562.
29. Pinkard, B., et al., *Review of Gasification of Organic Compounds in Continuous-Flow, Supercritical Water Reactors.* 2018.
30. Mourits, F.M. and F.H. Rummens, *A critical evaluation of Lennard–Jones and Stockmayer potential parameters and of some correlation methods.* Canadian Journal of Chemistry, 1977. **55**(16): p. 3007-3020.
31. Lemmon, E.W., M.O. McLinden, and D.G. Friend, ***NIST Chemistry WebBook, NIST Standard Reference Database Number 69***, E.P.J. Linstrom and W.G. Mallard, Editors.: Gaithersburg MD.
32. *ANSYS® Academic Research Fluent, Release 18.2*.
33. Spalart, P.R., et al., *A New Version of Detached-eddy Simulation, Resistant to Ambiguous Grid Densities.* Theoretical and Computational Fluid Dynamics, 2006. **20**(3): p. 181.
34. Sau, R. and K. Mahesh, *Dynamics and mixing of vortex rings in crossflow.* Journal of Fluid Mechanics, 2008. **604**.
35. Guan, Y. and I. Novosselov, *Damkohler Number Analysis in Lean Blow-Out of Toroidal Jet Stirred Reactor*. Journal of Engineering for Gas Turbines and Power, March 2018. **Accepted no. GTP-17-1495**.
36. Karalus, M.F., et al. *Characterizing the mechanism of lean blowout for a recirculation-stabilized premixed hydrogen flame*. in *ASME Turbo Expo 2012: Turbine Technical Conference and Exposition*. 2012. American Society of Mechanical Engineers.
37. Novosselov, I.V. and P.C. Malte, *Development and application of an eight-step global mechanism for CFD and CRN simulations of lean-premixed combustors.* Journal of Engineering for Gas Turbines and Power, 2008. **130**(2): p. 021502.